Appendix PDF contents

Appendix Figure Legends

Appendix Figure S1. HAT1 knockout HepG2 cell lines are established by the CRISPR-Cas9 system

A. The expression levels of HAT1 were measured by Western blot analysis in 48 cell clones derived from HepG2 cells #1-#24 clones came from the SgRNA1-selected cells, and #25-#48 clones came from the SgRNA2-selected cells.

B. Three clones were selected by length polymorphisms of PCR product and validated by Sanger sequencing. Clone #3 and Clone #20, Clone #34 were generated by SgRNA1 and SgRNA2 that produced Clone #3 with 1-bp deletion and 2+bp insertion, 4-bp deletion and 1+bp insertion for Clone #20 and 2+bp and 1+bp insertion for two alleles of Clone #34 at different positions, respectively.

Appendix Figure S2. HAT1 is able to modulate succinylation on multiple proteins

A. Total cell lysates from wild type (WT) and HAT1 knockout (KO) Clone 2 HepG2 cells were analyzed by Western blot analysis with the indicated pan-anti-Ksucc antibody and pan-anti-Kac antibody for Ksucc and Kac levels. The efficiency of HAT1 knockout was measured by Western blot analysis.

B. The levels of succinyl-CoA were analyzed by ELISA assays in HepG2 cells and HAT1 KO HepG2 cells. N = 3 biological replicates. Data were presented as mean ± SD. Student's *t*-test, ns, no significance.

C. Total cell lysates from wild type (WT) and HAT1 knockout (KO) Clone 1 HepG2 cells were analyzed by Western blot analysis with the indicated antibodies for Kac, lysine butyrylation (Kbu), lysine crotonylation (Kcr), and lysine propionylation (Kpr) levels. The efficiency of HAT1 knockout was measured by Western blot analysis.

Appendix Figure S3. Succinylation quantitative proteomics identify proteins and sites of HAT1-mediated succinylation

A. The schematic representation of the experimental workflow for the succinylation quantitative proteomics of HAT1-regulated succinylation was shown.

B. Venn diagram revealed the overlap between replications of the succinylation quantitative proteomics.

C. Histogram showed the Ksucc site distribution in the succinylation quantitative proteomics.

D. The consensus sequence logos demonstrated enrichment of amino acid residues among the HAT1-targeted Ksucc sites in the succinylation quantitative proteomics.

Appendix Figure S4. HAT1-mediated succinylation is involved in multiple biological processes and pathways

A-D. The succinylated proteins targeted by HAT1 were involved in many processes of physiology and pathology in the succinylation quantitative proteomics.

A. GO function enrichment analysis showed cellular biological process, molecular function, and cellular component with succinylated proteins targeted by HAT1.

B. Histogram revealed the relative fold change of Ksucc levels in the succinylation quantitative proteomics.

C. KEGG analysis showed the canonical pathway with succinylated proteins targeted by HAT1 in the succinylation quantitative proteomics.

D. Protein domain analysis demonstrated the specific domain of succinylated proteins targeted by HAT1 in the succinylation quantitative proteomics.

Appendix Figure S5. HAT1 is a novel histone succinyltransferase

A. Histones were extracted from HepG2 (WT) and HAT1 knockout (KO) Clone 2 HepG2 cells. The total histone succinylation and acetylation levels were analyzed by Western blot analysis in the cells. The histone levels were measured by GelCode Blue staining. The efficiency of HAT1 knockout was measured by Western blot analysis.

B. Histone H3 was immunoprecipitated from HepG2 cells with or without endogenous HAT1 depletion (by knockout). The levels of succinylation, acetylation, histone H3, HAT1, and β-actin were analyzed by Western blot analysis in the cells.

C. The efficiency of HAT1 shRNAs was validated by Western blot analysis in 293T cells

transfected with indicated shHAT1. Three shRNAs targeting HAT1 mRNA were designed, among which shHAT1-3 showed the strongest knockdown efficiency and was used in the following experiments.

D, E. Histone H3 was immunoprecipitated from PANC1 and HuCCT1 cells with or without endogenous HAT1 depletion (by shRNA). The levels of succinylation, acetylation, histone H3, HAT1, and β-actin were analyzed by Western blot analysis in the cells.

F. HAT1-catalyzed histone H3 acylation was analyzed by *in vitro* acylation assays using Western blot analysis after mixing purified HAT1, histone H3, and succinyl-CoA/butyryl-CoA/crotonyl-CoA/propionyl-CoA.

Appendix Figure S6. T188 of HAT1 is critical for HAT1-mediated succinylation

A. Two-dimensional (2D) diagram showed the catalytic pocket of HAT1 that bound to succinyl-CoA.

B. Histone H3 proteins were immunoprecipitated from HAT1 KO HepG2 cells, and HAT1 KO HepG2 cells re-expressed with HAT1 or indicated HAT1 mutants. The levels of succinylation, acetylation, histone H3, HAT1, and β-actin were determined by Western blot analysis in the cells.

C, D. The steady-state kinetics of HAT1-mediated histone H3 modifications was shown. Immunoprecipitated wild type Flag-HAT1 or Flag-HAT1 (T188A) from 293T cells was incubated with purified histone H3 in the presence of acetyl-CoA or succinyl-CoA. The steady-state kinetics of HAT1 activity was determined by measuring CoA production. The *K*m values of wild type Flag-HAT1 for histone H3 acetylation and succinylation were 1.08 ± 0.14

μM (means ± S.D.) and 0.61 ± 0.10 μM, respectively. The *K*m values of Flag-HAT1 (T188A) for histone H3 acetylation and succinylation were 1.15 ± 0.14 μM and 1.57 ± 0.37 μM, respectively. The steady-state kinetic curves showed the mean values from three independent measurements (n=3). The *V*max values of wild type Flag-HAT1 for histone H3 acetylation and succinylation were 1.58 ± 0.05 nM s^{-1} (mean ± S.D.) and 1.75 ± 0.07 nM s^{-1}, respectively. The *V*max values of Flag-HAT1 (T188A) for histone H3 acetylation and succinylation were 1.56 ± 0.05 nM s^{-1} and 0.68 ± 0.04 nM s^{-1}, respectively. The data were presented as means ± S.D. from three independent experiments (n=3). N = 3 biological replicates. Data were presented as mean ± SD. Student's *t*-test, ***$P<0.001$; ns, no significance.

E, F. Histone H3 was immunoprecipitated from PANC1 and HuCCT1 cells depleted endogenous HAT1 and in the cells reconstituted expression of HAT1 or HAT1 mutant (T188A). The levels of succinylation, acetylation, histone H3, HAT1, and β-actin were analyzed by Western blot analysis in the cells.

G. Histone H3 was immunoprecipitated from HepG2, HAT1 KO Clone 1 HepG2, and HAT1 KO Clone 1 HepG2 cells reconstituted expression of HAT1 or HAT1 mutant (T188A). The levels of succinylation, acetylation, butyrylation, crotonylation, propionylation, histone H3, HAT1, and β-actin were analyzed by Western blot analysis.

Appendix Figure S7. HAT1 catalyzes histone H3K122 succinylation for epigenetic regulation

A. The diagram showed the succinylated histone sites identified in the succinylation quantitative proteomics.

B. The diagram showed the ratios of histone succinylation sites targeted by HAT1 in the succinylation quantitative proteomics.

C. The levels of histone H3K122 succinylation, histone H3K122 acetylation, histone H3K27 acetylation, histone H3, HAT1, and β-actin were determined by Western blot analysis in HepG2, HAT1 knockout (KO) Clone 2 HepG2 cells, and in the cells reconstituted expression of HAT1 or HAT1 mutant (T188A).

D. The levels of histone H3K122 succinylation, histone H3K27 acetylation, histone H3, HAT1, and β-actin were examined by Western blot analysis in PANC1, and PANC1 cells depleted endogenous HAT1, or HuCCT1 and HuCCT1 cells depleted endogenous HAT1.

E. The levels of histone H3K122 succinylation, histone H3K27 acetylation, histone H3, HAT1, and β-actin were examined by Western blot analysis in PANC1, or HuCCT1 cells depleted endogenous HAT1, and in the cells reconstituted expression of HAT1 or HAT1 mutant (T188A).

F. HAT1-mediated histone H3K122 succinylation was analyzed by mixing purified HAT1, histone H3, and succinyl-CoA (2 μM) with or without acetyl-CoA (2 μM). Western blot analysis was performed with the indicated antibodies.

G. The H3K122succ-ChIP peaks and HAT1-ChIP peaks were identified by ChIP-seq in HepG2 cells. Venn diagram showed the overlap of H3K122 succinylation and HAT1 common occupied peaks.

H. The diagram showed the genomic distributions of ChIP-seq peaks for H3K122 succinylation and HAT1 in HepG2 cells.

Appendix Figure S8. Representative tracks of gene peaks from H3K122 succinylation ChIP-seq

A. The representative tracks of gene peaks from H3K122 succinylation ChIP-seq were showed.

Appendix Figure S9. HAT1 catalyzes histone H3K122 succinylation for gene expression regulation

A, B. The effect of HAT1 on histone H3K122 succinylation and histone H3K122 acetylation at the indicated gene promoters was determined by ChIP assay with an anti-H3K122 succinylation antibody and anti-H3K122 acetylation antibody, and quantitative PCR with primers of the promoter regions of CREBBP, BPTF and RPTOR in PANC1/HuCCT1 cells, PANC1/HuCCT1 cells depleted endogenous HAT1, and PANC1/HuCCT1 cells depleted endogenous HAT1 and reconstituted expression of HAT1 or HAT1 mutant (T188A). N = 3 biological replicates. Data were presented as mean ± SD. Student's *t*-test, ***$P<0.001$; ns, no significance.

C, D. The mRNA levels of CREBBP, BPTF, and RPTOR were measured by RT-qPCR in PANC1/HuCCT1 cells, PANC1/HuCCT1 cells depleted endogenous HAT1 and PANC1/HuCCT1 cells depleted endogenous HAT1 and reconstituted expression of HAT1 or HAT1 mutant (T188A). N = 3 biological replicates. Data were presented as mean ± SD. Student's *t*-test, **$P<0.01$.

E. The levels of histone H3K122 succinylation, histone H3K79 succinylation, histone H3K9 acetylation, histone H3, KAT2A, and β-actin were assessed by Western blot analysis in

HepG2 and HepG2 cells depleted endogenous KAT2A. The levels of histone H3K79 succinylation, histone H3K27 acetylation, histone H3, HAT1, and β-actin were assessed by Western blot analysis in HepG2 and HepG2 cells depleted endogenous HAT1.

Appendix Figure S10. The interaction analysis of HAT1-modulated succinylation

A. The interaction analysis showed that HAT1-mediated succinylation targeted glycolysis.

Appendix Figure S11. HAT1-mediated non-histone succinylation specifically targets glycolysis

A, B. The decrease of glucose and increase of lactate in culture medium were measured by ELISA assays in PANC1/HuCCT1 cells, PANC1/HuCCT1 cells depleted endogenous HAT1, and PANC1/HuCCT1 cells depleted endogenous HAT1 and reconstituted expression of HAT1 or HAT1 mutant (T188A). N = 3 biological replicates. Data were presented as mean ± SD. Student's *t*-test, $^{**}P<0.01$.

C-F. The relative amounts of indicated metabolites were quantified by ELISA assays in PANC1/HuCCT1 cells, PANC1/HuCCT1 cells depleted endogenous HAT1, and PANC1/HuCCT1 cells depleted endogenous HAT1 and reconstituted expression of HAT1 or HAT1 mutant (T188A). N = 3 biological replicates. Data were presented as mean ± SD. Student's *t*-test, $^{**}P<0.01$; ns, no significance.

Appendix Figure S12. HAT1 modulates succinylation of PGAM1

A. PGAM1 was immunoprecipitated from HepG2, HAT1 KO Clone 2 HepG2, and HAT1 KO

Clone 2 HepG2 cells reconstituted expression of HAT1 or HAT1 mutant (T188A). The levels of succinylation, PGAM1, HAT1, and β-actin were analyzed by Western blot analysis in the cells.

B. PGAM1 was immunoprecipitated from PANC1/HuCCT1, PANC1/HuCCT1 cells depleted endogenous HAT1, and PANC1/HuCCT1 cells depleted endogenous HAT1 and reconstituted expression of HAT1 or HAT1 mutant (T188A). The levels of succinylation, PGAM1, HAT1, and β-actin were analyzed by Western blot analysis in the cells.

C. ENO1 or PKM was immunoprecipitated from HepG2, HAT1 KO HepG2, and HAT1 KO HepG2 cells reconstituted expression of HAT1 or HAT1 mutant (T188A). The levels of succinylation, ENO1 or PKM, HAT1, and β-actin were analyzed by Western blot analysis in the cells.

D. The relative enzyme activity of PGAM1, ENO1, and PKM was measured by the enzyme activity assays in the indicated tumor cells. N = 3 biological replicates. Data were presented as mean ± SD. Student's *t*-test, $^{*}P<0.05$; $^{**}P<0.01$.

E. PGAM1 was immunoprecipitated from HepG2, HAT1 KO Clone 1 HepG2, and HAT1 KO Clone 1 HepG2 cells reconstituted expression of HAT1 or HAT1 mutant (T188A). The levels of succinylation, acetylation, butyrylation, crotonylation, propionylation, PGAM1, HAT1, and β-actin were analyzed by Western blot analysis.

F. The effect of HAT1 on histone H3K122 succinylation and histone H3K122 acetylation at PGAM1 promoter was determined by ChIP assays with anti-H3K122 succinylation antibody and anti-H3K122 acetylation antibody, and followed by quantitative PCR with primer of the promoter region of PGAM1 in WT HepG2 cells, HAT1 KO HepG2 cells and HAT1 KO

HepG2 cells reconstituted expression of HAT1 or HAT1 mutant (T188A). N = 3 biological replicates. Data were presented as mean ± SD. Student's *t*-test, ns, no significance.

G. The mRNA levels of PGAM1 were measured by RT-qPCR in HepG2 cells, HAT1 KO HepG2 cells, and HAT1 KO HepG2 cells reconstituted expression of HAT1 or HAT1 mutant (T188A). N = 3 biological replicates. Data were presented as mean ± SD. Student's *t*-test, ns, no significance.

Appendix Figure S13. HAT1 is able to directly succinylate PGAM1

A, B. The decrease of 2-PG and increase of 3-PG were measured by ELISA assays in PANC1/HuCCT1 cells, PANC1/HuCCT1 cells depleted endogenous HAT1, and PANC1/HuCCT1 cells depleted endogenous HAT1 and reconstituted expression of HAT1 or HAT1 mutant (T188A). N = 3 biological replicates. Data were presented as mean ± SD. Student's *t*-test, $^{**}P<0.01$.

C. HAT1-catalyzed PGAM1 acylation was analyzed by *in vitro* acylation assays using Western blot analysis after mixing purified HAT1, PGAM1, and succinyl-CoA/butyryl-CoA.

D. HAT1-catalyzed PGAM1 acylation was analyzed by *in vitro* acylation assays using Western blot analysis after mixing purified HAT1, PGAM1, and succinyl-CoA/crotonyl-CoA.

E. HAT1-catalyzed PGAM1 acylation was analyzed by *in vitro* acylation assays using Western blot analysis after mixing purified HAT1, PGAM1, and succinyl-CoA/ propionyl-CoA.

F. HAT1-catalyzed PGAM1 succinylation was analyzed by mixing purified HAT1 and

succinyl-CoA, and purified PGAM1 or PGAM1 mutant in the *in vitro* succinylation assays. Western blot analysis was performed with indicated antibodies.

Appendix Figure S14. HAT1 succinylates PGAM1 to enhance glycolysis

A. The purified HAT1, PGAM1, and succinyl-CoA were mixed in the *in vitro* succinylation assays. And the relative PGAM1 activity was measured by the PGAM1 activity assays *in vitro*. N = 3 biological replicates. Data were presented as mean ± SD. Student's *t*-test, $^{**}P<0.01$.

B. The relative activity of PGAM1 and PGAM1 mutant (K to E) were analyzed by the PGAM1 activity assays *in vitro*. N = 3 biological replicates. Data were presented as mean ± SD. Student's *t*-test, $^{**}P<0.01$.

C. The efficiency of PGAM1 shRNAs was validated by Western blot analysis in 293T cells transfected with indicated shPGAM1. Three shRNAs targeting PGAM1 mRNA were designed, among which shPGAM1-2 showed the strongest knockdown efficiency and was used in the following experiments.

D, E. The decrease of glucose and increase of lactate in the culture medium and the relative amounts of 2-PG and 3-PG were analyzed by ELISA assays in PANC1/HuCCT1 cells depleted endogenous PGAM1 and reconstituted expression of PGAM1 or PGAM1 mutant (K99R). N = 3 biological replicates. Data were presented as mean ± SD. Student's *t*-test, $^{**}P<0.01$.

Appendix Figure S15. HAT1-mediated succinylation displays critical roles in tumor

growth

A-E. PANC1 cells, PANC1 cells depleted endogenous HAT1, and PANC1 cells depleted endogenous HAT1 and reconstituted expression of HAT1 or HAT1 mutant (T188A), were subcutaneously injected into athymic nude mice (N=6).

A, B. Photographs showed the tumors from the nude mice. Tumor volumes and average tumor weight were calculated. N = 6 biological replicates. Data were presented as mean ± SD. Student's *t*-test, ***$P<0.001$.

C. Immunohistochemical analysis of the indicated tumor sections was performed with an anti-Ki67 antibody. The images represented the results of six tissue slides.

D. Western blot analysis was performed with the indicated antibodies. Representative images of triplicate experiments were shown.

E. The relative amounts of 3-PG and 2-PG were determined by ELISA assays in the tumor tissues. N = 6 biological replicates. Data were presented as mean ± SD. Student's *t*-test, **$P<0.01$.

Appendix Figure S16. The succinylation of PGAM1 plays a crucial role in tumor growth

A-E. PANC1 cells depleted endogenous PGAM1 and reconstituted expression of PGAM1, or PGAM1 mutant (T188A) were subcutaneously injected into athymic nude mice (N=6).

A, B. Photographs showed the tumors from the nude mice. The average tumor weight and

tumor volumes were calculated. N = 6 biological replicates. Data were presented as mean ± SD. Student's *t*-test, ***$P<0.001$.

C. Immunohistochemical analysis of the indicated tumor sections was performed with an anti-Ki67 antibody. The images represented the results of six tissue slides.

D. Western blot analysis was performed with the indicated antibodies. Representative images of triplicate experiments were shown.

E. The relative amounts of 3-PG and 2-PG were determined by ELISA assays in the tumor tissues. N = 6 biological replicates. Data were presented as mean ± SD. Student's *t*-test, ***$P<0.001$.

Appendix Figure S17. Histone acetyltransferase 1 is a succinyltransferase for histones and non-histones in liver cancer

A model of succinylation mediated by HAT1. As a writer, HAT1 affects Ksucc levels on various proteins, including histones and non-histones, which is involved in multiple cellular pathways of physiology and pathology. For histones, HAT1 is a novel histone succinyltransferase and enhances epigenetic regulation and gene expression profiling by catalyzing histone H3K122 succinylation. For non-histones, HAT1 facilitates glycolysis through catalyzing the succinylation of PGAM1 on K99 in tumor cells. Functionally, HAT1-mediated succinylation is essential for the progression of liver cancer.

Yang G, et al. Appendix Figure S1

A

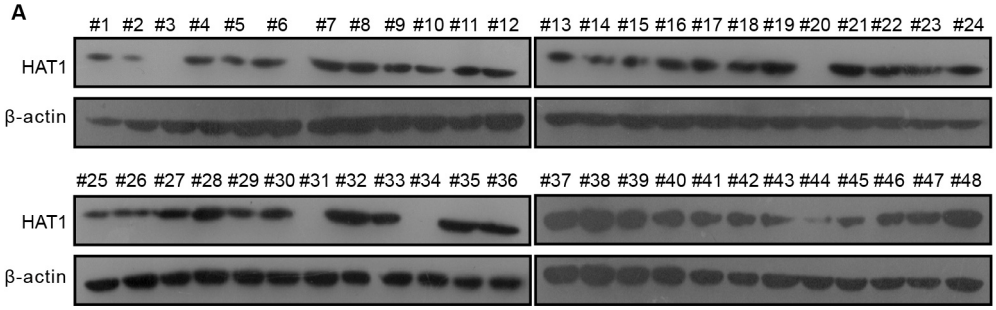

B

SgRNA1 Site	TCCC**TAGGCTGACATGACATGTAG**AGGCTTT	Indels
Clone#3 (Clone 1)	TCCC**TAGGCTGACATGACA**····**GTAG**AGGCTTT	-1bp
	TCCC**TAGGCTGACATGACAT**G**G**C**TAG**AGGCTTT	+2bp

SgRNA1 Site	TCCC**TAGGCTGACATGACATGTAG**AGGCTTT	Indels
Clone#20 (Clone 2)	TCCC**TAGGCTGACATGA**····**TAG**AGGCTTT	-4bp
	TCCC**TAGGCTGACATGACAT**T**GTAG**AGGCTTT	+1bp

SgRNA2 Site	TGGA**GCTACGCTCTTTGCGACCGT**AGGCTAC	Indels
Clone#34	TGGA**GCTACGCTCTTTGCGAC**T**G**A**CGT**AGGCTAC	+2bp
	TGGA**GCTACGCTCTTTGCGA**T**CCGT**AGGCTAC	+1bp

Yang G, et al. Appendix Figure S2

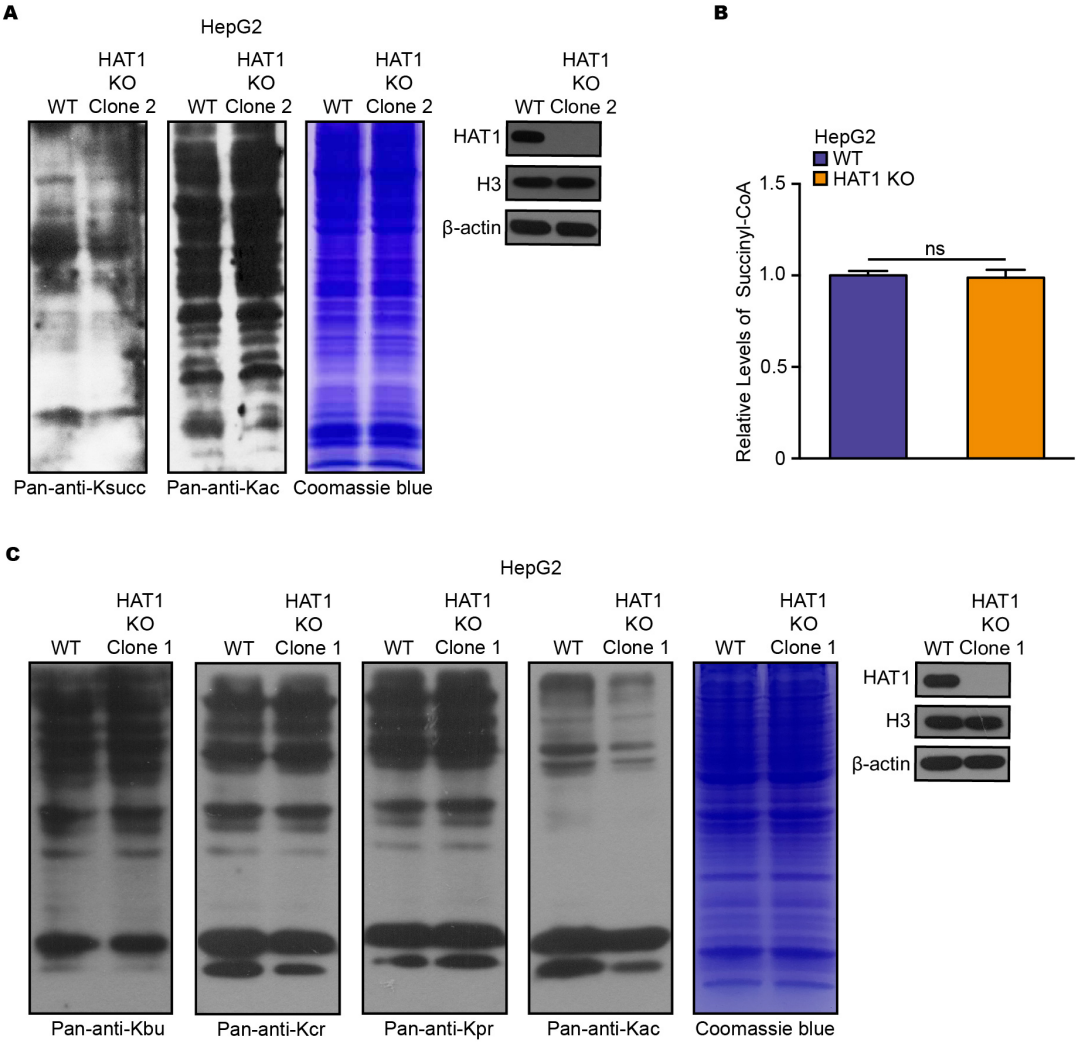

Yang G, et al. Appendix Figure S3

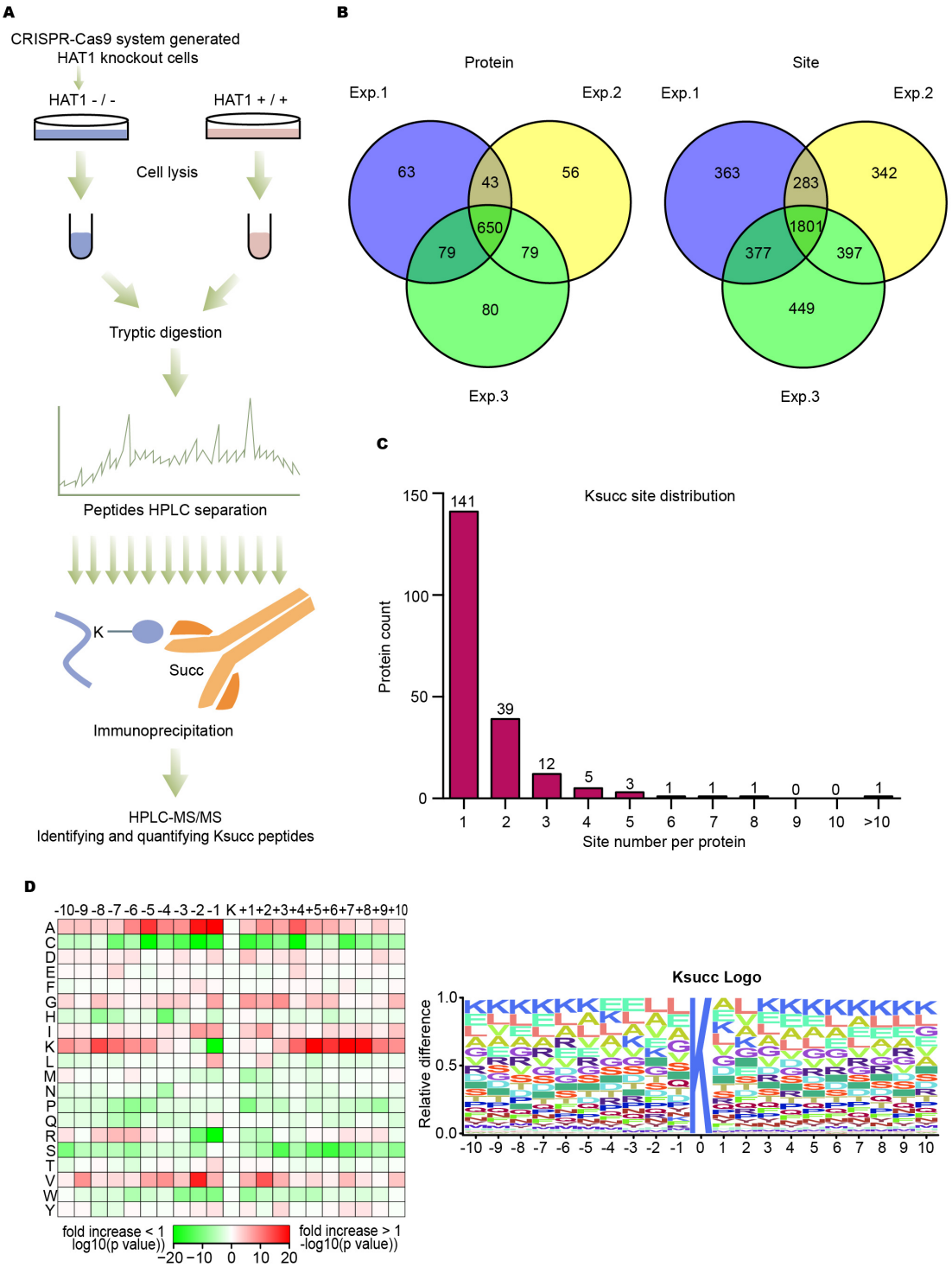

Yang G, et al. Appendix Figure S4

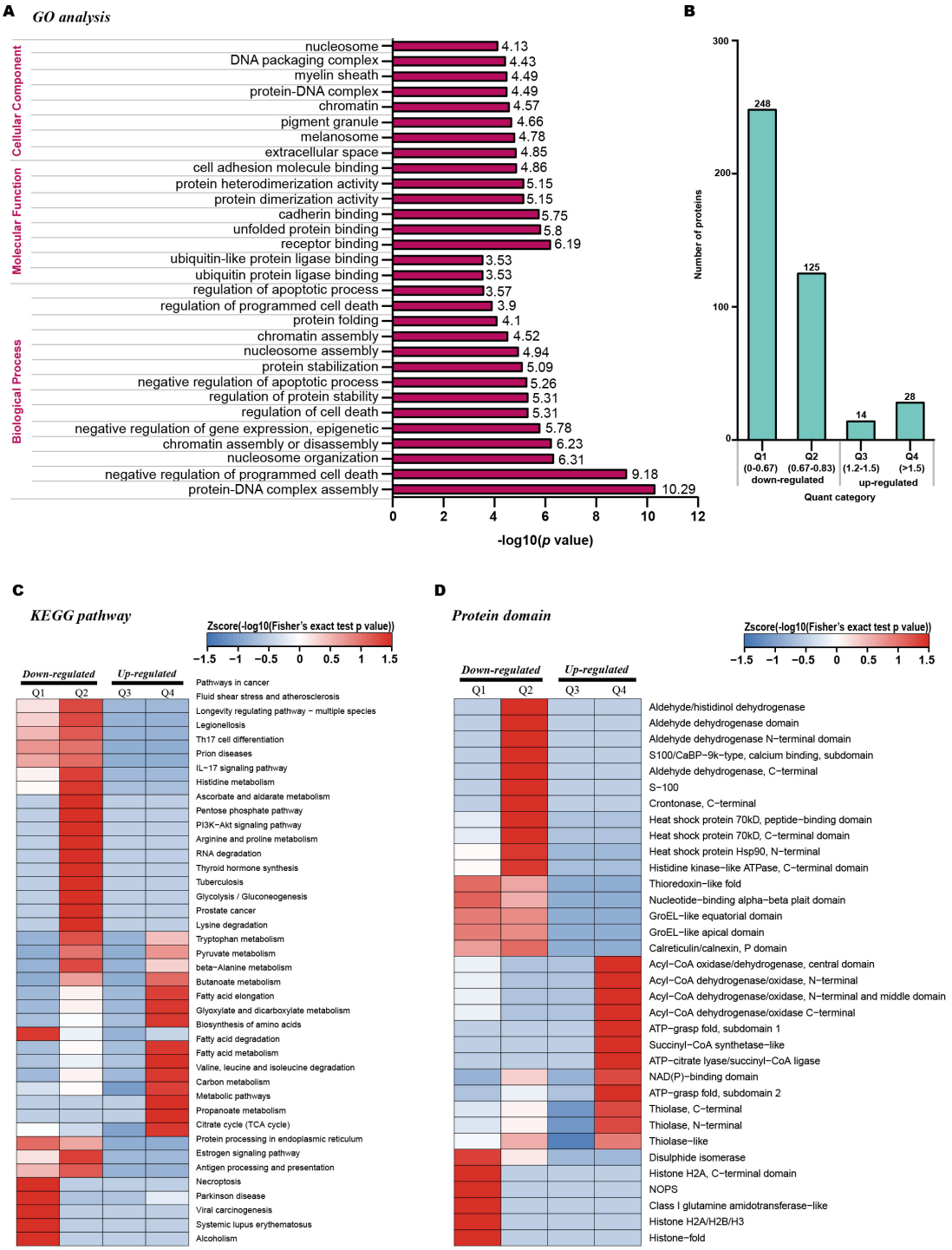

Yang G, et al. Appendix Figure S5

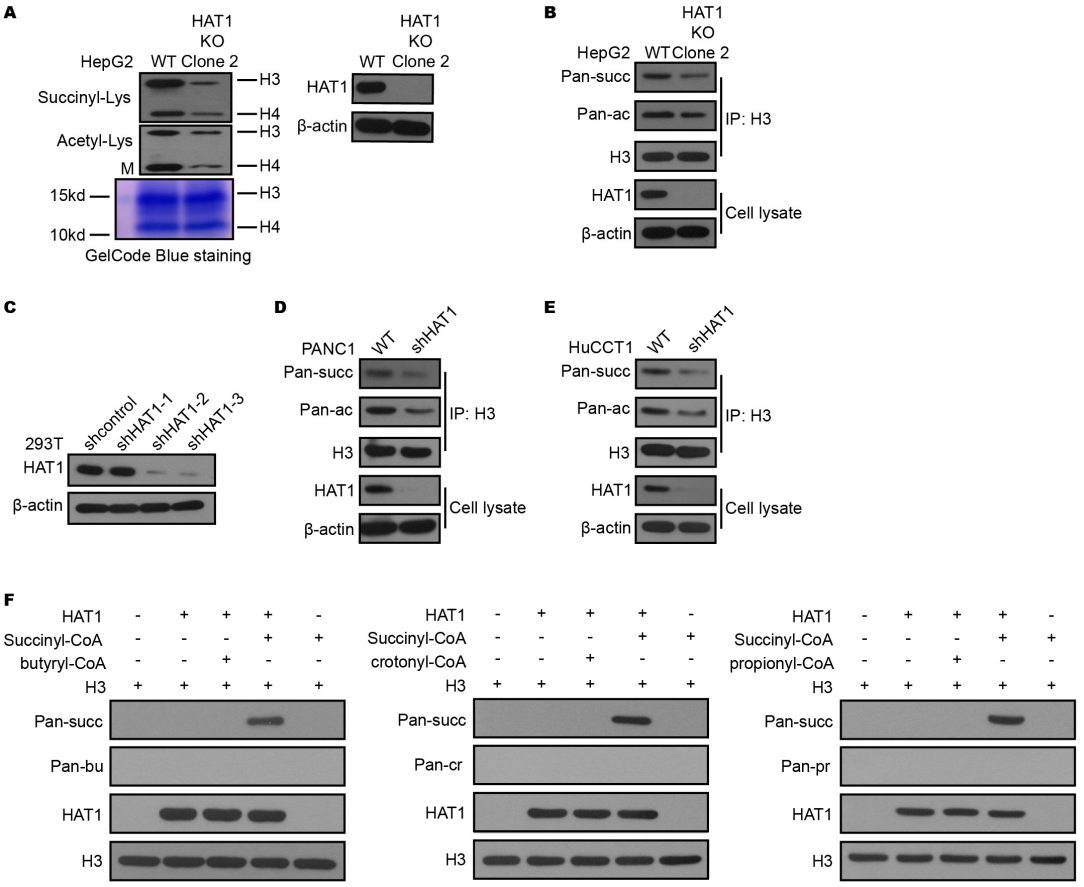

Yang G, et al. Appendix Figure S6

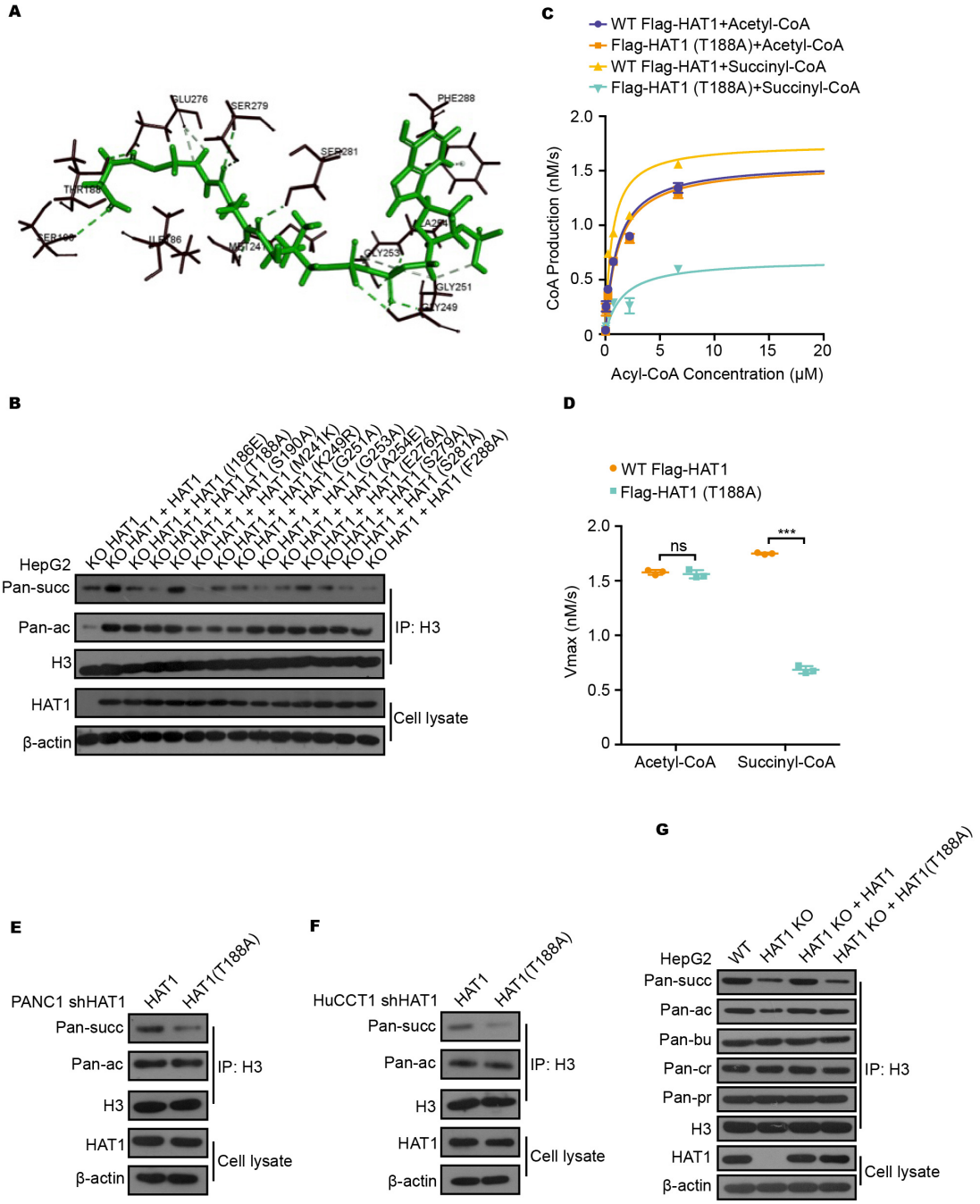

Yang G, et al. Appendix Figure S7

A

Representative Ksucc sites of histones identified in this study

H3

New identify

+H_3N-ARTKQTARKSTGG**K**APRKQLAT**K**AARKSAPATGGV**K**KPHRYRPGTV...Q**K**ST... IRKL...FKTDLRFQSS...DTN...AKR...P**K**D...ARRIRG ERA-COO-

14 23 36 56 122

H4

AcHN-SGRGKGG**K**GLG**K**GGAKRHRKVLRDNIQGIT**K**PAIRR...VKRISGLIYEETRGVLKV...VIRDAVTYTEHA**K**R**K**TVTAMDVV YALKRQG RTLYGFGG-COO-

8 12 31 77 79

H2A

AcHN-SGRGKQGGKARAKAKTRSSRAG LQFPVGRVHRLLRKGNYAERV...PVYL...LTA...ARDNKKT...IRNDEELN**K**LLGKVTI...LLPKKTESHHKAKGK-COO-

95

H2B

+H3N-PEPA**K**SA...P**K**KGSKKAVT**K**AQKKD...RKRSR**K**E SYS...Y**K**VL**K**...TGISSK...S...SEASRLAHYN**K**RSTITSRE...VRL ...A**K**H...GT**K**AVT**K**YTSAK-COO-

5 11 20 34 43 46 85 108 116 120

H1

+H3N-SETA...EKAPVKKKAAKKAGGTPRKA SGPPVSELITKAVAASKERSGVSLAAL**KK**AL...GYDVEKNNSRIKLGLKSLVS**K**GTLVQTKGTGASGSF**K**LNK

63 64 89 105

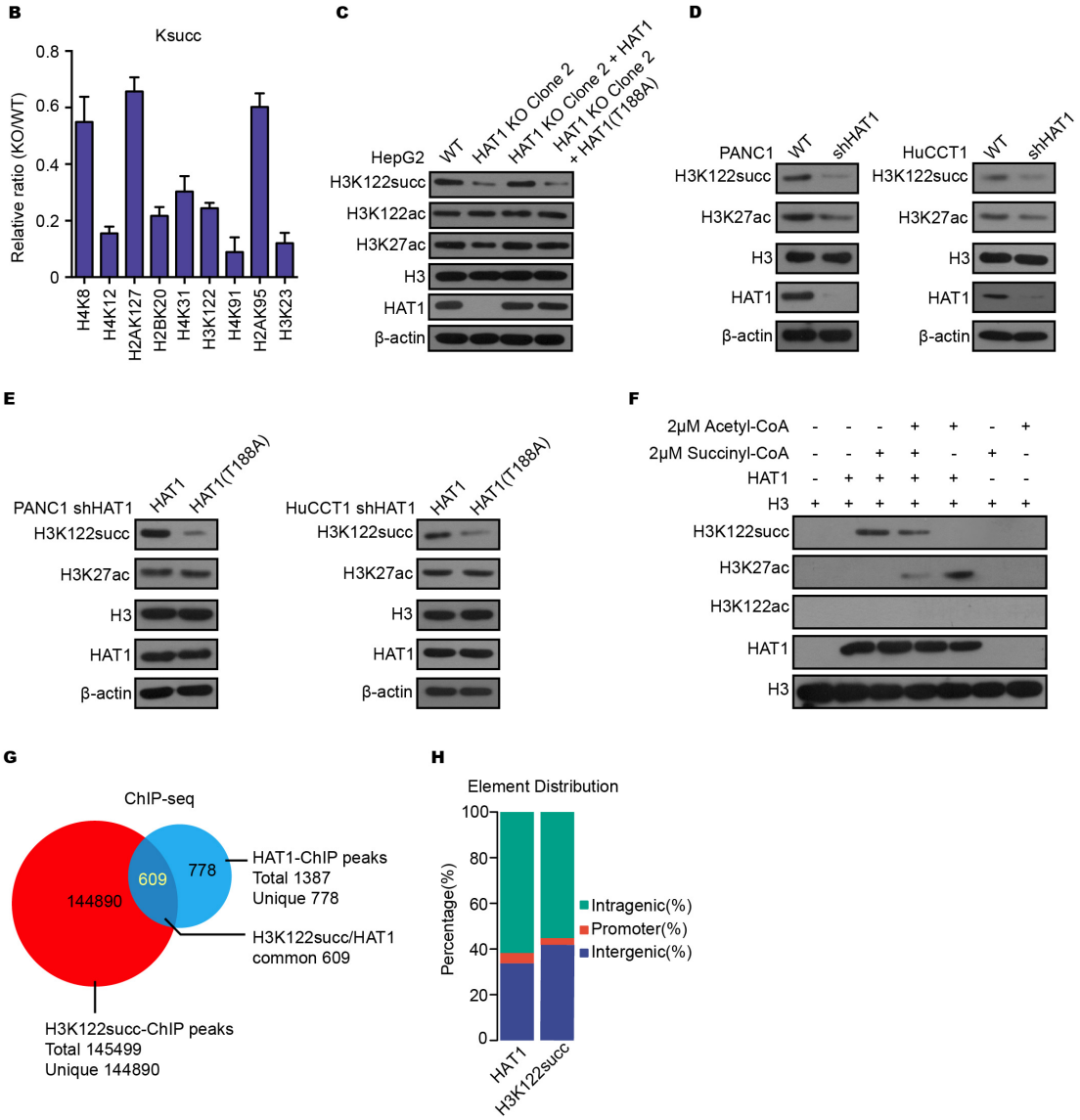

Yang G, et al. Appendix Figure S8

A

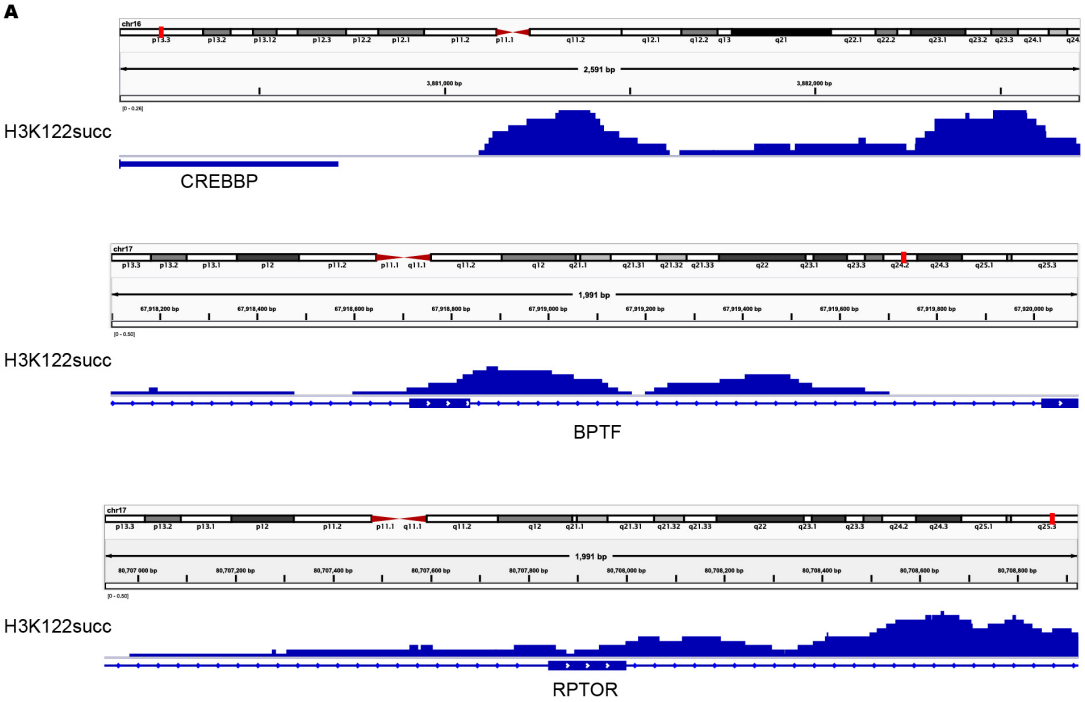

Yang G, et al. Appendix Figure S9

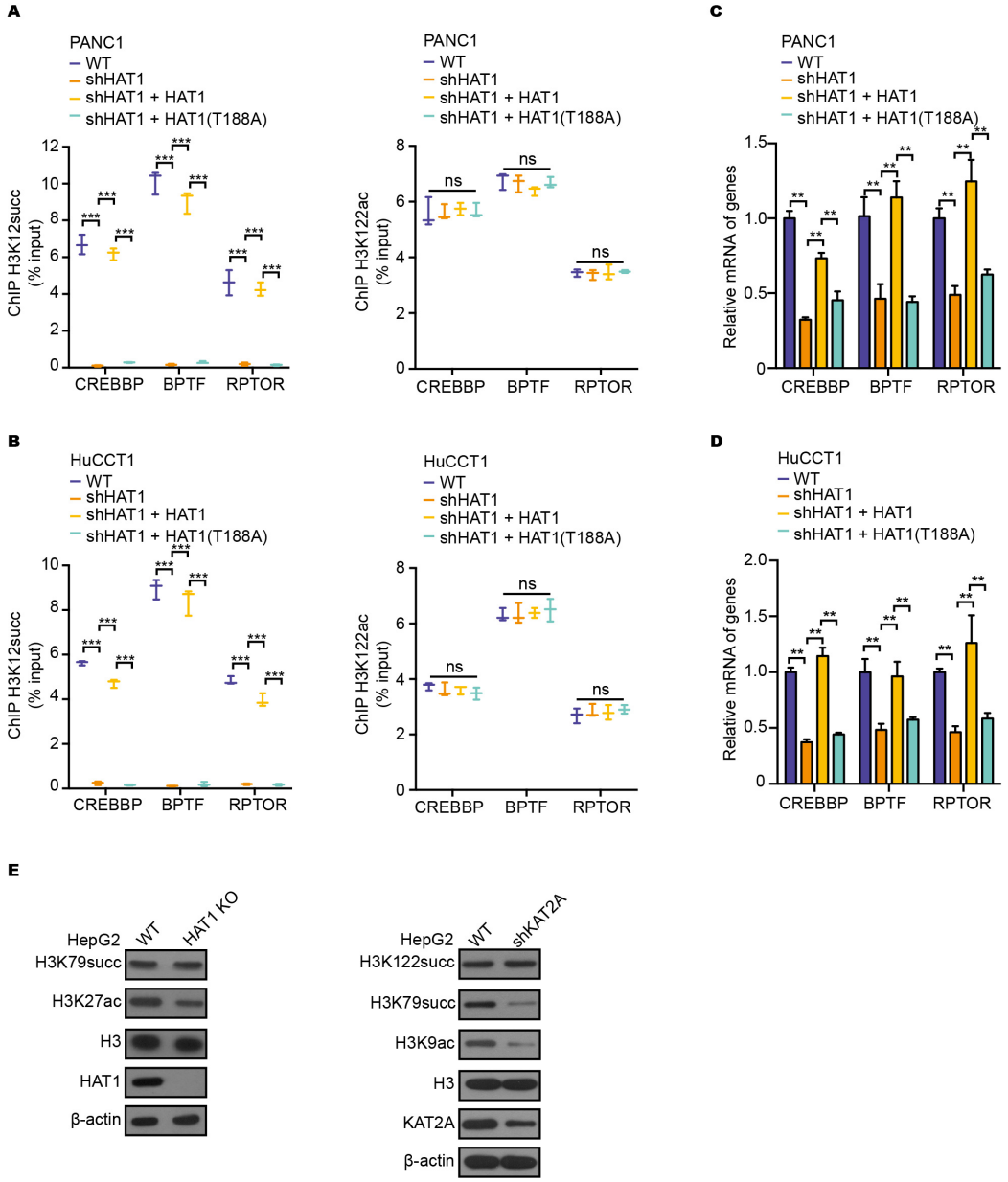

Yang G, et al. Appendix Figure S10

A

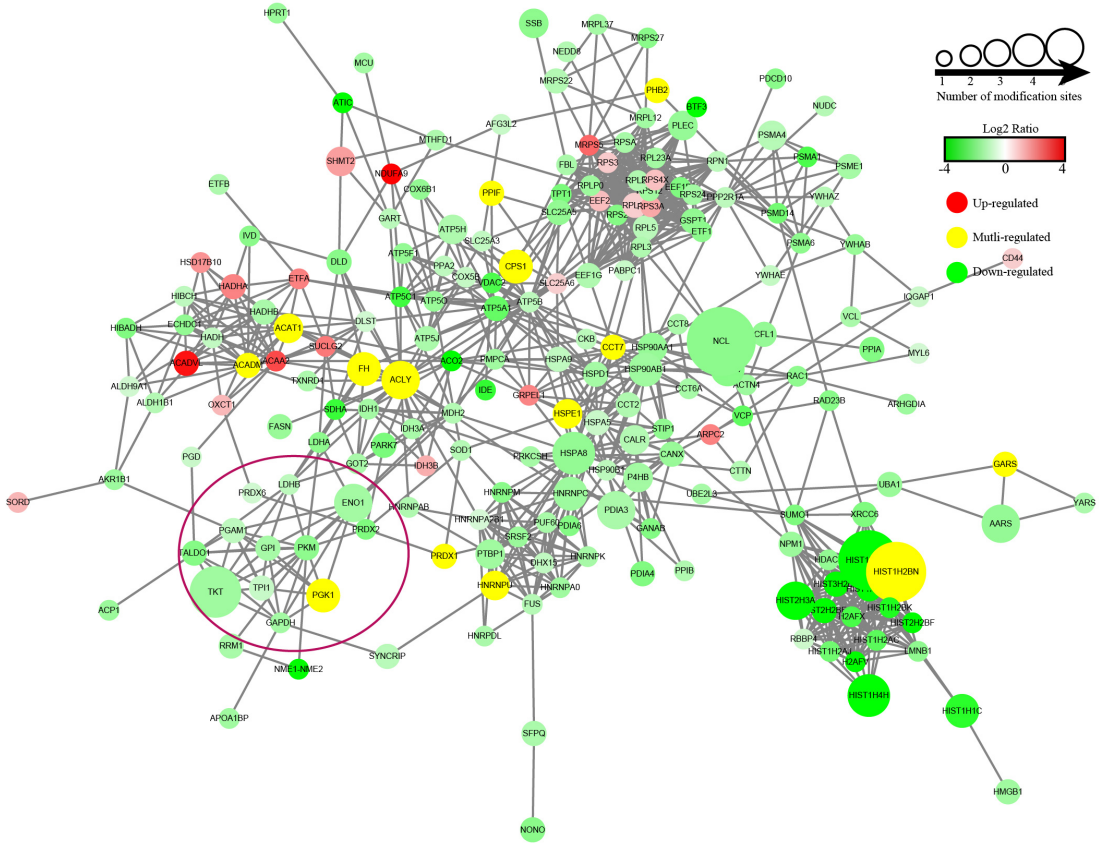

Yang G, et al. Appendix Figure S11

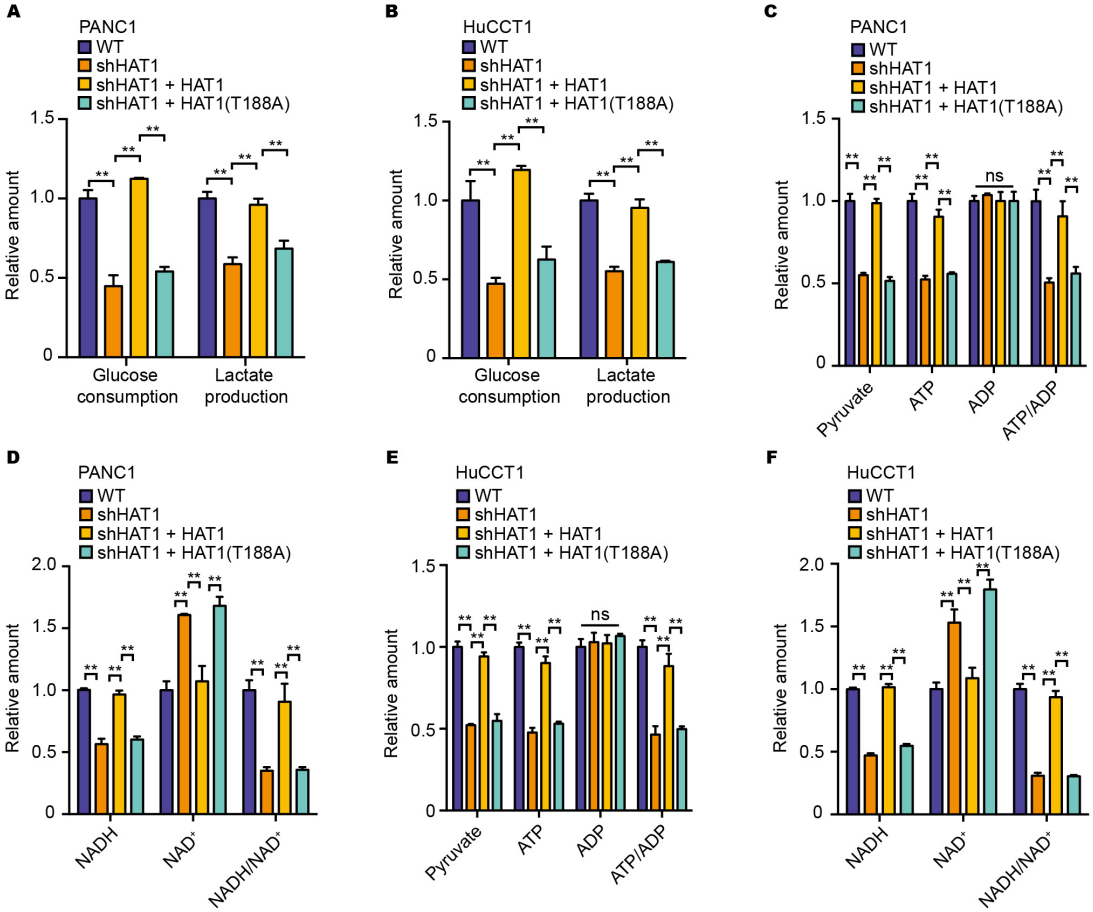

Yang G, et al. Appendix Figure S12

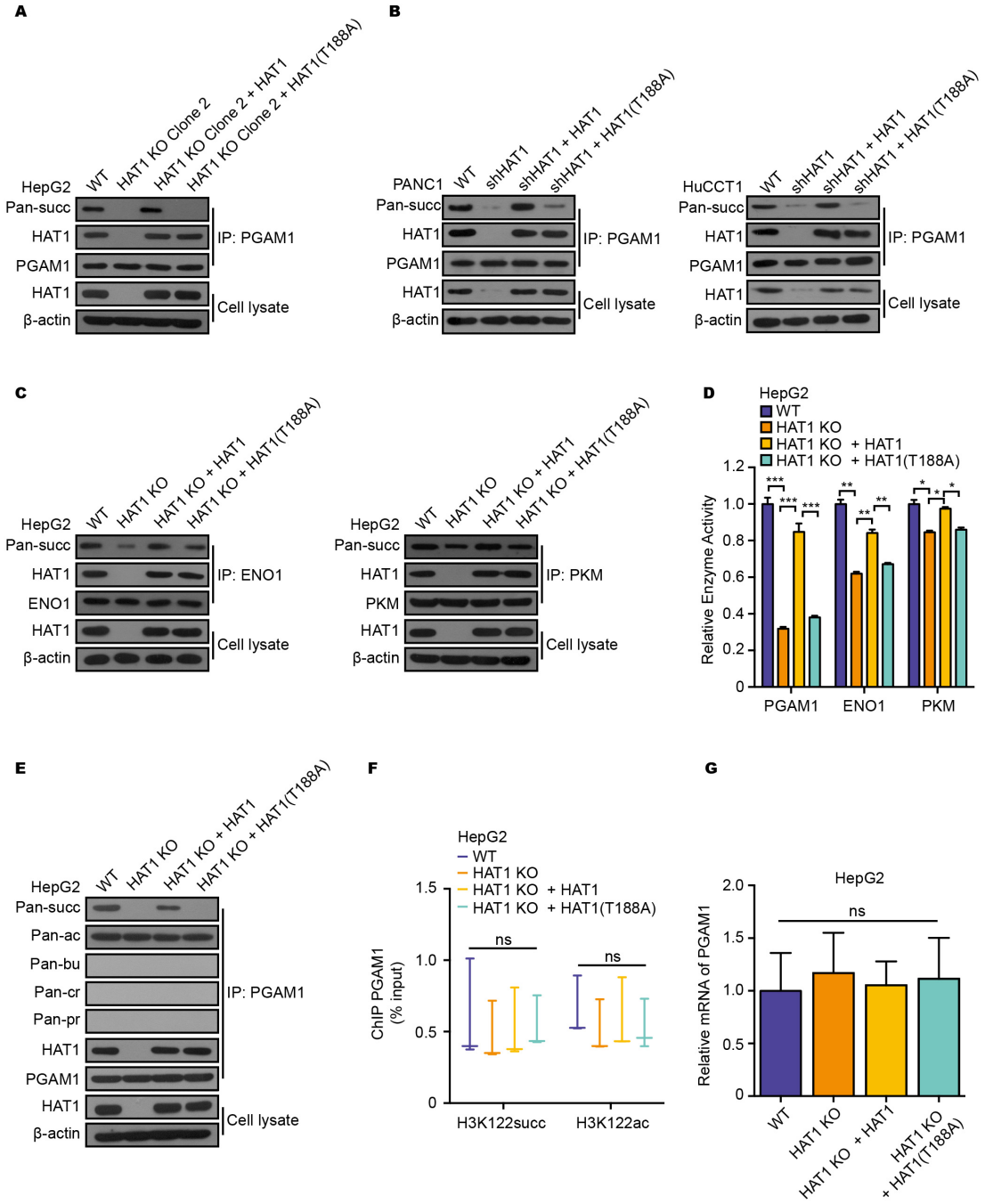

Yang G, et al. Appendix Figure S13

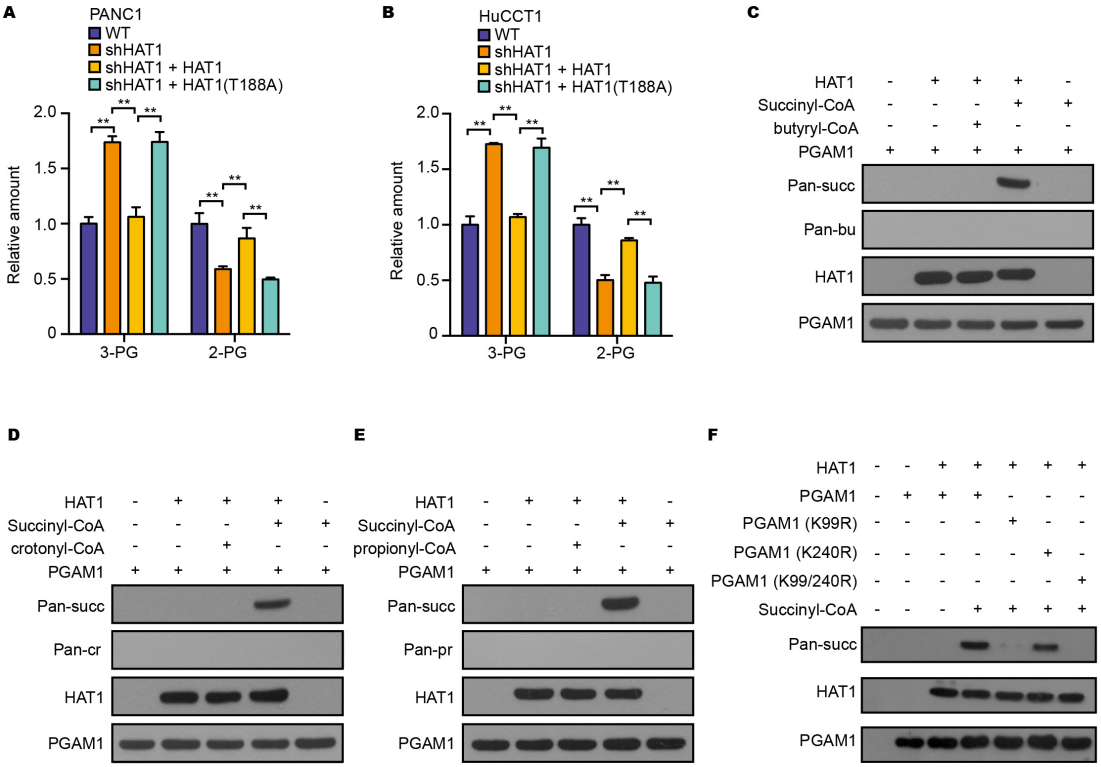

Yang G, et al. Appendix Figure S14

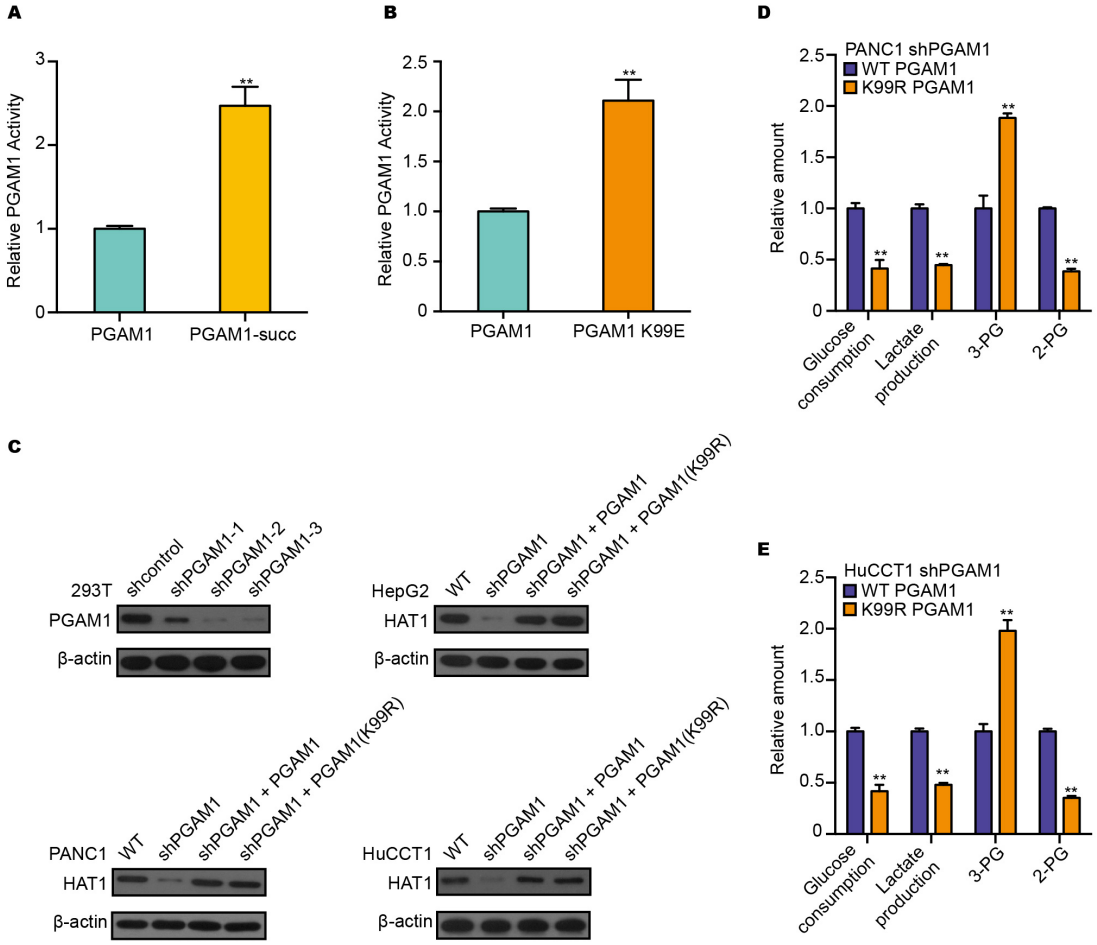

Yang G, et al. Appendix Figure S15

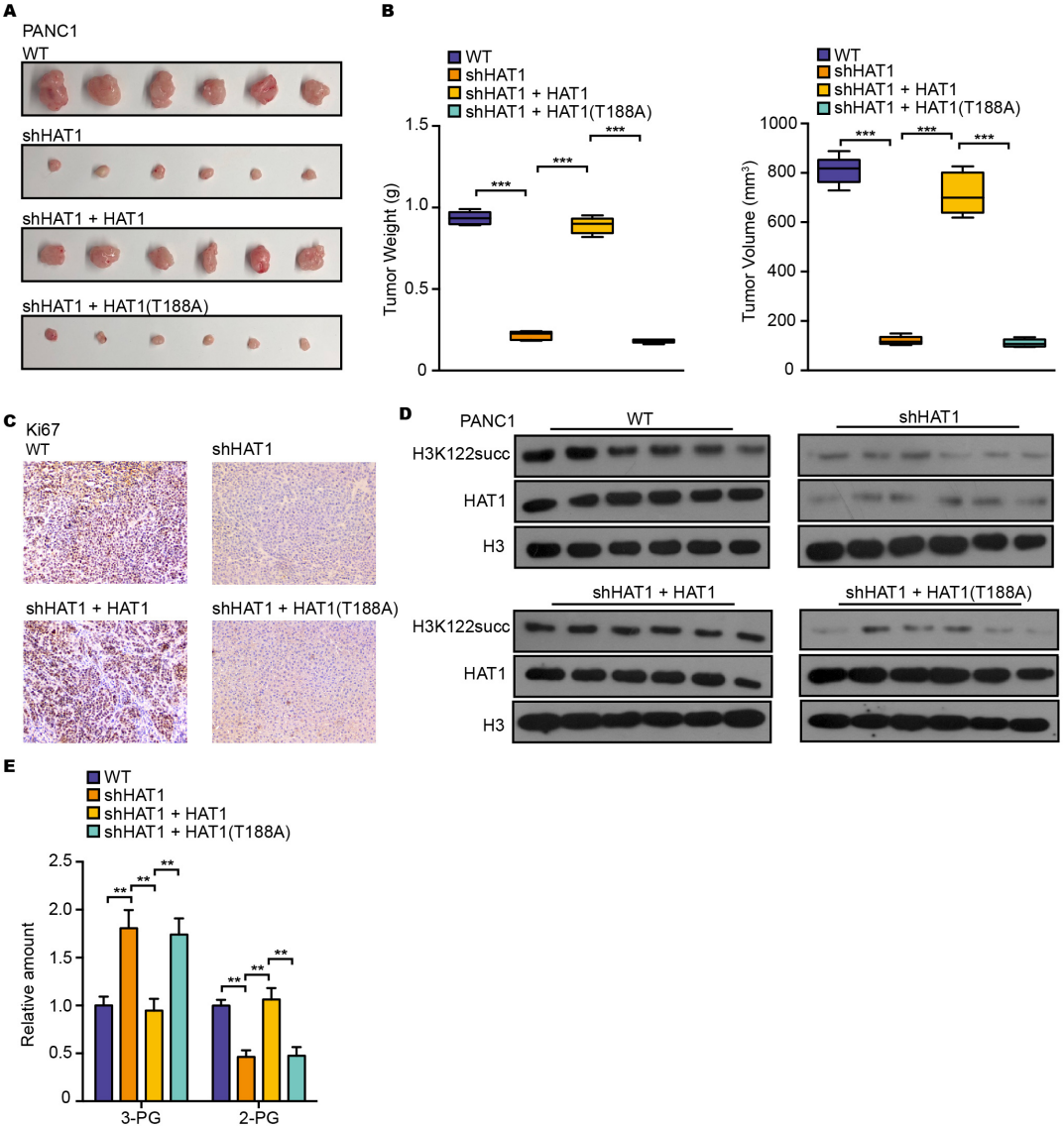

Yang G, et al. Appendix Figure S16

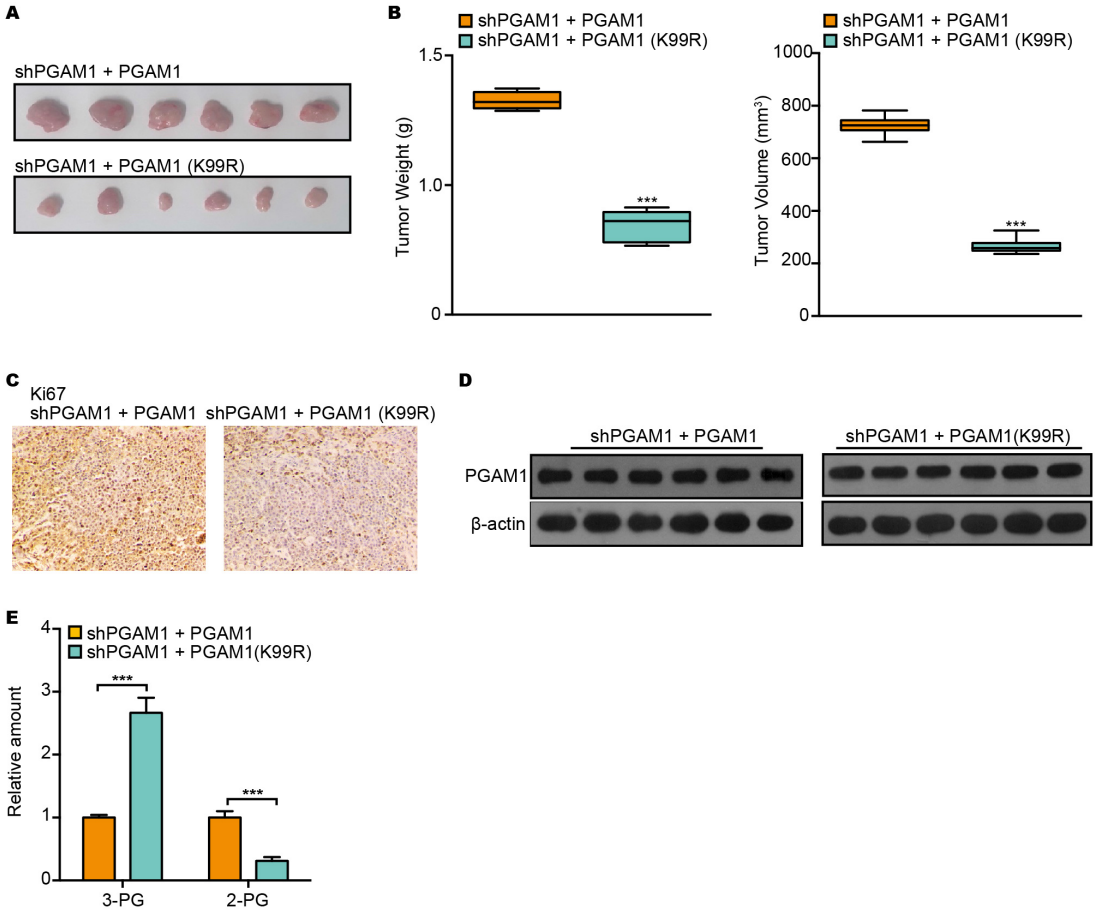

Yang G, et al. Appendix Figure S17

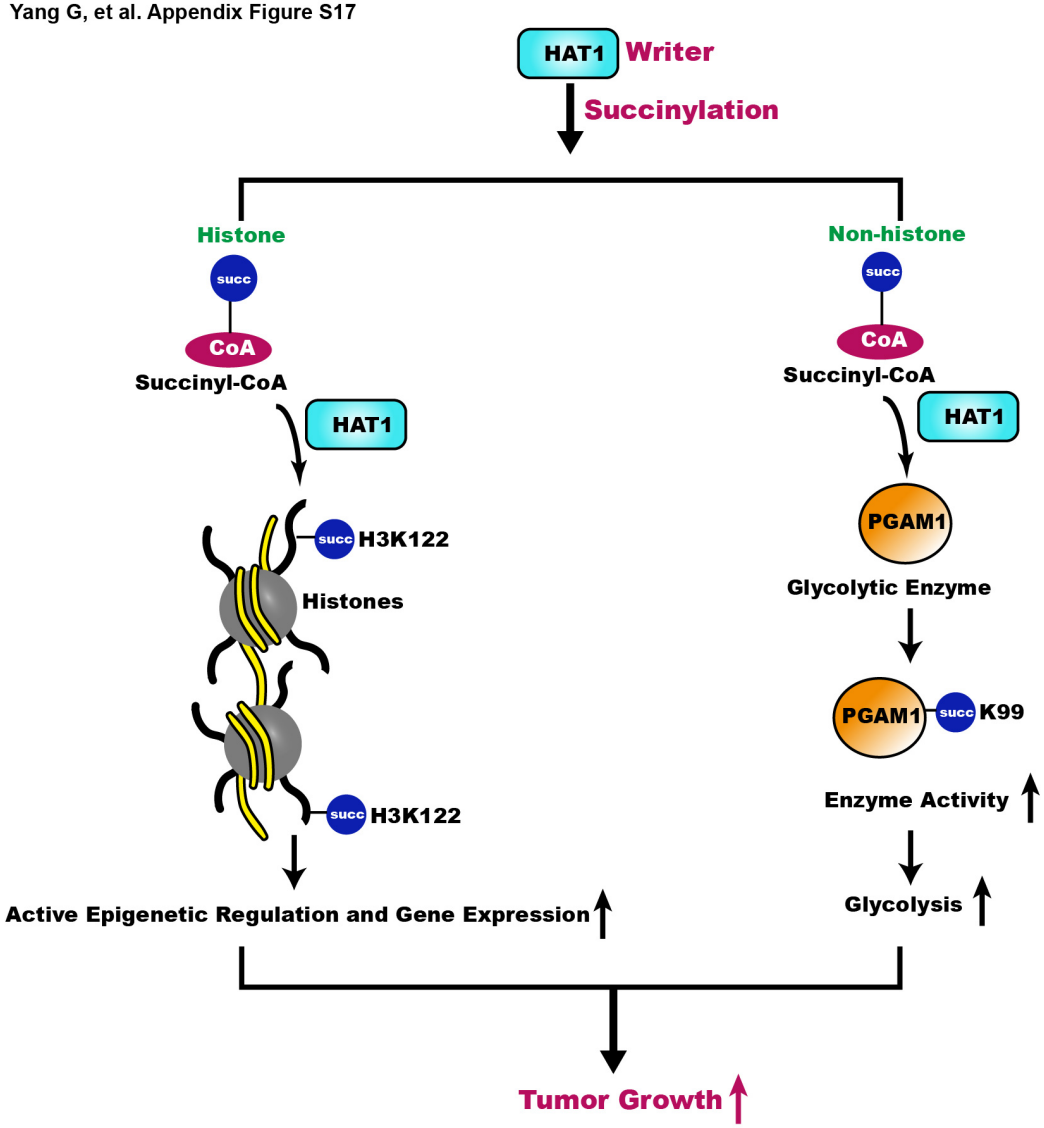

Appendix Table S1: target sequences of shRNAs

shRNAs	Target sequence (5′-3′)
shHAT1-1	GCGTGTTATTGAACGACTTGC
shHAT1-2	GGTCTAAAGATCCTGTTATAC
shHAT1-3	GCTACAGACTGGATATTAA
shPGAM1-1	TTTCTGCTTTATTGAGACCGG
shPGAM1-2	ATGTTGCTGTAGAAAGGATGG
shPGAM1-3	CCATCCTTTCTACAGCAACAT
shKAT2A-1	CGTGCTGTCACCTCGAATGA

Appendix Table S2: Primer list

Gene	Forward and reverse primer (5′-3′)
PCR	
CREBBP mRNA	TGAGAACTTGCTGGACGGAC
	CACTGAGGCTGGCCATGTTA
BPTF mRNA	CCCAGGTGGTGATGAAGCAT
	TTCTGACACCGATCACAGCC
RPTOR mRNA	TCTGTCGGCATCTTCCCCTA
	CCAGCTCGCTGTCCACTG
PGAM1 mRNA	TTGAATACAGCGACCCAGTGG
	CTATCGATGTACAGCCGAATGGTG
GAPDH	ACCAACTGCTTAGCCC
	CCACGACGGACACATT
CREBBP promoter	CTAGTGTCACGAGGTAGGGC
	GGAATGGCCTCTGCAGGTTA
BPTF promoter	TCAGGGTTGAGTCGCTGTGA
	AGAGAGACAAGCCCCCTGAA
RPTOR promoter	ACAAGAGGCTTGCCTCCAC
	CCGACAGACCAAACCTCCTC
PGAM1 promoter	CACCTCTCCAGTTACTAAATTCCAT
	CTGTTCTTCTCCGAGCCCCAATCAG
Plasmid construction	
HAT1-WT	CGCGGATCCATGGCGGGATTTGGTGCTATGG
	CCGCTCGAGTTACTCTTGAGCAAGTCGTTCA
HAT1 (I186E)	GCTTCAGACCTTTTTGATGTGGTTTGAGGAAACTGCTAGCTTTATTGACGTGG
	CCACGTCAATAAAGCTAGCAGTTTCCTCAAACCACATCAAAAAGGTCTGAAGC
HAT1 (T188A)	GACCTTTTTGATGTGGTTTATTGAAGCTGCTAGCTTTATTGACGT
	ACGTCAATAAAGCTAGCAGCTTCAATAAACCACATCAAAAAGGTC
HAT1 (S190A)	TGATGTGGTTTATTGAAACTGCTGCCTTTATTGACGTGGATGATGAAAG
	CTTTCATCATCCACGTCAATAAAGGCAGCAGTTTCAATAAACCACATCA
HAT1 (M241K)	GCCACGTGTAAGTCAGAAGCTGATTTTGACTCCAT
	ATGGAGTCAAAATCAGCTTCTGACTTACACGTGGC
HAT1 (K249R)	TGATTTTGACTCCATTTCAAGCTCAAGGCCATGGTGC
	GCACCATGGCCTTGAGCTTGAAATGGAGTCAAAATCA
HAT1 (G251A)	TCCATTTCAAGGTCAAGCCCATGGTGCTCAACTTC
	GAAGTTGAGCACCATGGGCTTGACCTTGAAATGGA
HAT1 (G253A)	TTCAAGGTCAAGGCCATGCTGCTCAACTTCTTGAA
	TTCAAGAAGTTGAGCAGCATGGCCTTGACCTTGAA

HAT1 (A254E)	CAAGGTCAAGGCCATGGTGAACAACTTCTTGAAACAGTTC
	GAACTGTTTCAAGAAGTTGTTCACCATGGCCTTGACCTTG
HAT1 (E276A)	AGTTCTTGATATTACAGCGGCAGATCCATCCAAAAGCTATG
	CATAGCTTTTGGATGGATCTGCCGCTGTAATATCAAGAACT
HAT1 (S279A)	ATATTACAGCGGAAGATCCAGCCAAAAGCTATGTGAAATTACG
	CGTAATTTCACATAGCTTTTGGCTGGATCTTCCGCTGTAATAT
HAT1 (S281A)	CAGCGGAAGATCCATCCAAAGCCTATGTGAAATTACGAGACT
	AGTCTCGTAATTTCACATAGGCTTTGGATGGATCTTCCGCTG
HAT1 (F288A)	AAGCTATGTGAAATTACGAGACGCTGTGCTTGTGAAGCTTTGTCAAG
	CTTGACAAAGCTTCACAAGCACAGCGTCTCGTAATTTCACATAGCTT
PGAM1-WT	CGCGGATCCATGGCCGCCTACAAACTGGTG
	CCGCTCGAGTCACTTCTTGGCCTTGCCCTG
PGAM1 (K99E)	GGGTCTAACCGGTCTCAAAAAAGCAGAAACTGCTG
	CAGCAGTTTCTGCTTTTTTGAGACCGGTTAGACCC
CRISPR/Cas9	
HAT1-sgRNA-1	GACCGTAGGCTGACATGACATGTAG
	AAACCTACATGTCATGTCAGCCTAC
HAT1-sgRNA-2	GACCGGCTACGCTCTTTGCGACCGT
	AAACACGGTCGCAAAGAGCGTAGCC

Appendix Table S3: antibodies used in this study

Antibodies	Origin	Applications
HAT1	Proteintech 11432-1-AP	Western blot
HAT1	Abcam ab194296	IP, ChIP
H3	Abcam ab1791	Western blot, IP
Pan Kac	PTMBIO PTM-105	Western blot,
Pan Kac	Abcam ab21623	IP
Pan Ksucc	PTMBIO PTM-419	Western blot, IP
Pan Bu	PTMBIO PTM-301	Western blot, IP
Pan Pr	PTMBIO PTM-201	Western blot, IP
Pan Cr	PTMBIO PTM-501	Western blot, IP
H3K122succ	PTMBIO PTM-413	Western blot, ChIP
H3K79succ	PTMBIO PTM-412	Western blot
H3K27ac	Abcam ab4729	Western blot
H3K122ac	Affinity AF4362	Western blot, ChIP
PGAM1	Proteintech 16126-1-AP	Western blot, IP
ENO1	Proteintech 55237-1-AP	Western blot, IP
PKM	Proteintech 25659-1-AP	Western blot, IP
IgG Polyclonal Antibody	Abcam ab6789	ChIP, IP
Flag tag Monoclonal Antibody	Sigma-Aldrich SAB4200071	IP
Ki-67 Polyclonal Antibody	Proteintech 27309-1-AP	IHC
His-Tag Monoclonal Antibody	Proteintech 66005-1-Ig	IP
β-actin Monoclonal Antibody	Sigma-Aldrich A2228	Western blot

Appendix Table S4: Stoichiometry of succinylation on glycolytic enzymes

Protein	Succinylation site	Stoichiometry in HepG2 cells (mean, %)	Stoichiometry in HAT1-knockout HepG2 cells (mean, %)
PGAM1	K99	62.0	47.1
PGAM1	K240	26.3	18.1
ENO1	K232	53.9	38.4
PKM	K310	20.7	13.0
PGK1	K352	21.2	12.7
GPI	K123	18.8	12.7
GAPDH	K226	9.4	6.0
TPI	K178	49.5	40.7